Title:
# Shape Accuracy in the Forming of Deep Holes with Retreat and Advance Pulse Ram Motion on a Servo Press

Authors:
Ryo Matsumoto[1,*], Jae-Yeol Jeon[1] and Hiroshi Utsunomiya[1]

* Corresponding author (R. Matsumoto, E-mail: ryo@mat.eng.osaka-u.ac.jp, Tel: +81-6-6879-7500, Fax: +81-6-6879-7500)

Affiliation:
[1] Division of Materials and Manufacturing Science, Graduate School of Engineering, Osaka University, 2-1 Yamadaoka, Suita 565-0871, Japan

**Abstract**

A method for keeping lubrication in the backward extrusion of deep holes for lightweight structural components is proposed utilizing a servo press and a punch with an internal channel for liquid lubricant supply. The punch is pushed into the specimen with a servo press in a manner that combines pulsed and stepwise modes. Sufficient liquid lubricant is periodically supplied to the deformation zone through the internal channel upon the retreat of the punch. The appropriate punch motions for prevention of galling of the formed hole for extrusion ratios in the range 1.07–1.80 were determined in the proposed forming method using a servo press. Furthermore, the proposed method was found to produce the formed holes with high shape accuracy. The shape accuracy of the formed hole is discussed with experimental and finite element simulation results in terms of lubrication state and temperature change.

Keywords: Forging; Extrusion; Lubrication; Shape accuracy; Servo press

## 1. Introduction

Since the ram speed and motion of servo presses can be programmed with a servomotor through CNC control, servo presses have led to new forming processes (Ernst, 2011; Osakada et al., 2011). For example, Wang et al. (2009) have controlled the product shape in free forging for artificial bones with a servo press and a 6-axis freedom robot. Groche et al. (2010) have developed a 3D servo press to realize flexible forming processes. Maeno et al. (2011) have reduced the friction in cold plate forging through load pulsation using a servo press.

Forged products are desired with high accuracy in the shape. The desire has been gradually strict in net shape cold forging process. Shape accuracy of the forged product is complexly determined by many forging parameters such as forging temperature, strain, friction and rigidity of the dies and so on. Although the control of these forging parameters is limited in conventional forging process using a mechanical press, servo presses with flexible ram motion are useful to control temperature, strain and stress of billet and dies during forging. Ishiguro et al. (2010) have investigated the shape accuracy of the forged product under several press ram motions on a servo press, however the effective ram motions for obtaining the forged product with high shape accuracy have not been specified.

For the fabrication of lightweight components such as hollow components, we proposed an extrusion method for forming of deep holes that utilizes a punch with an internal channel for the supply of liquid lubricant using a servo press (Matsumoto et al., 2011). The concept of the proposed forming method is derived from the machining of deep holes with tools that have internal channels for lubricant. In machining, a drill with an internal channel for lubricant makes it possible to cut deep holes by supplying lubricant to the cutting part (Weinert et al., 2004). The proposed forming method has been confirmed to prevent galling in the backward extrusion of aluminium alloy under a low extrusion ratio, however, the

relationship between the extrusion ratio and the appropriate punch motions for prevention of galling and the accuracy of the shape of the formed specimen have not previously been investigated.

In this study, the appropriate punch motions for prevention of galling of the formed hole at several extrusion ratios are investigated with the proposed forming method using a servo press. The accuracy of the shape of the formed hole with the proposed forming method is examined and discussed in terms of lubrication and temperature changes through the experimental and finite element simulation results.

## 2. Extrusion with pulsating lubricant supply

### 2.1. Backward extrusion method

The proposed extrusion method for reducing the friction over the punch surface is shown in Fig. 1 (Matsumoto et al., 2011). The punch with an internal channel for lubricant flow is pushed into the specimen in a manner that combines pulsed and stepwise modes and assists the supply of liquid lubricant from the punch nose. The punch is connected to a lubricant tank, and the lubricant is supplied to the internal channel from the tank. During forming with a manner that combines pulsed and stepwise modes, the internal pressure in the cavity formed in the previous forming steps is depressurized by the retreat action of the punch, and the lubricant is sucked into the cavity through the internal channel (Fig. 1(b)). In this method, a pump and/or a check valve for prevention of flow backward is not used for supplying the lubricant from the punch nose. The lubricant is supplied to the deformation zone only by the change in the internal pressure in the cavity. After the retreat of the punch, the punch is advanced again to continue the forming of the hole (Fig. 1(c)). When sufficient lubricant is supplied to the cavity during the retreat of the punch, the forming of the hole can be carried out without seizure during the next advance of the punch (Fig. 1(c)). A hole with a

high aspect ratio can be formed without seizure by using a stepwise mode that consists of repeated retreats and advances of the punch.

To describe the punch motion, the following parameters are defined:

$n_{total}$: total number of forming steps

$s_{ai}$: advance stroke in the $i$-th forming step ($i$ = 1 to $n_{total}$)

$s_{ri}$: retreat stroke in the $i$-th forming step ($i$ = 1 to $n_{total}$)

$s_{fi}$: forming stroke in the $i$-th forming step (= $s_{ai}$–$s_{ri}$) ($i$ = 1 to $n_{total}$)

$s_{total}$: total forming stroke of the punch ($= \sum_{i=1}^{n_{total}} s_{fi}$)

In this study, $s_{ai}$, $s_{ri}$, and $s_{fi}$ were set as constant at each forming step. Thus, $s_{ai}$, $s_{ri}$, and $s_{fi}$ can be written as $s_a$, $s_r$, and $s_f$, respectively.

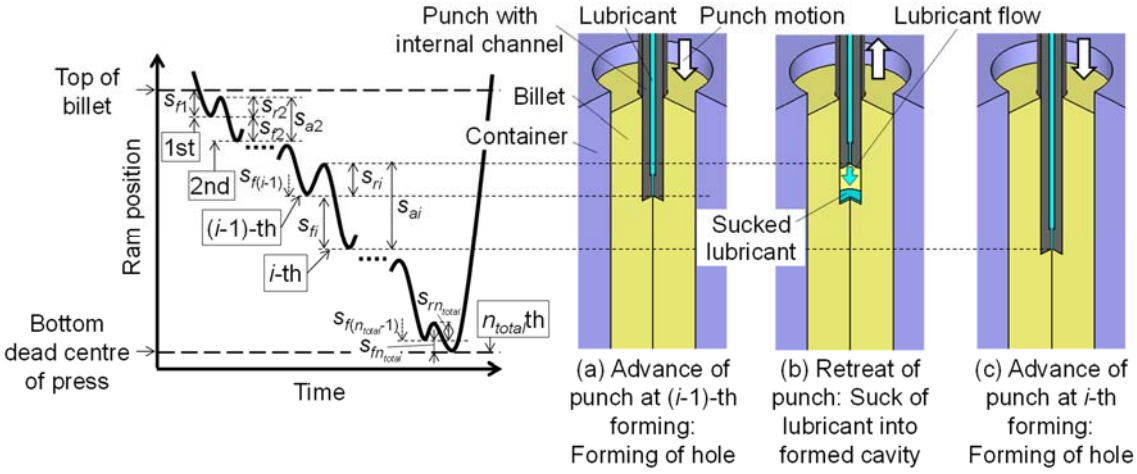


Fig. 1 Retreat and advance pulse ram motion of a punch with an internal channel for pulsating lubricant supply in backward extrusion ($s_{ai}$: advance stroke of punch at $i$-th forming, $s_{ri}$: retreat stroke of punch at $i$-th forming, $s_{fi}$: forming stroke of punch at $i$-th forming, $i$ = 1 to $n_{total}$).

## 2.2. Experimental conditions

The tool arrangement for the forming method is shown in Fig. 2. The punch with an internal channel for lubricant flow is connected to the lubricant tank by a tube. No equipment such as a pump or a valve to prevent backflow of lubricant was used. Mineral oil with a kinematic viscosity of 32 $mm^2/s$ (at 40 ºC) was used as the lubricant. The punch diameter is $D_P$ = 6.0 mm, and the diameters of the internal channel are $D_I$ = 1.5 and 0.5 mm. To vary the extrusion ratio ($R$) of the hole, containers with inner diameters $D_C$ = 24, 18, 12, and 9 mm were prepared. The outer diameter of the containers was 75 mm. The extrusion ratios are $R$ = 1.07, 1.13, 1.33, and 1.80, and the wall thicknesses of the formed specimens are 9, 6, 3, and 1.5 mm, respectively. The materials used for the punch and containers were cemented tungsten carbide (DIJET Industrial Co., Ltd., WC-10mass%Co) and matrix high speed tool steel (Hitachi Metals, Ltd., YXR3), respectively. Each punch and container surface was polished to a mirror finish with $Ra$ = 0.02–0.04 μm. The picture of the punch and container is shown in Fig. 3. The specimen material was an AA6061-T6 aluminium alloy. The tools were installed on a 450 kN servo press (Komatsu Industrial Corp., H1F45). The servo press was driven by an AC servomotor through a mechanical link (0–70 spm). The total step number ($n_{total}$) was limited to less than five because of the press specifications. The advance and retreat punch speeds–stroke diagram is shown in Fig. 4.

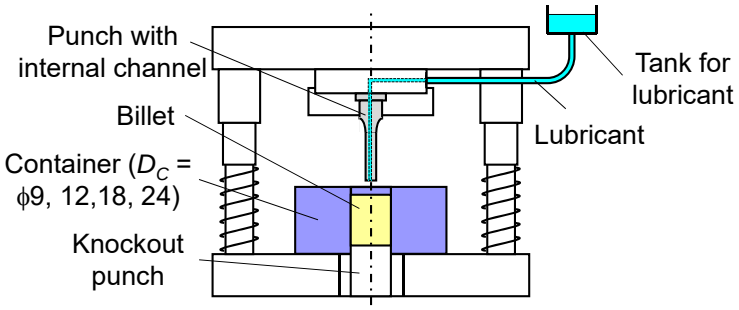


(a) Tool arrangement.

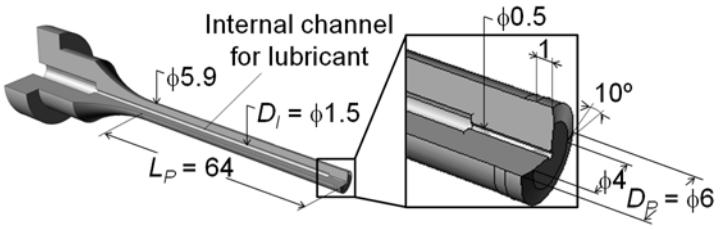


(b) Punch with an internal channel for lubricant supply.

Fig. 2 Schematic illustrations of the tool arrangement and a punch with an internal channel for lubricant supply ($D_C$: inner diameter of container, $D_P$: punch diameter, $D_I$: diameter of the internal channel, $L_P$: punch length).

Fig. 3 Picture of punch with an internal channel for lubricant supply (left) and container (right).

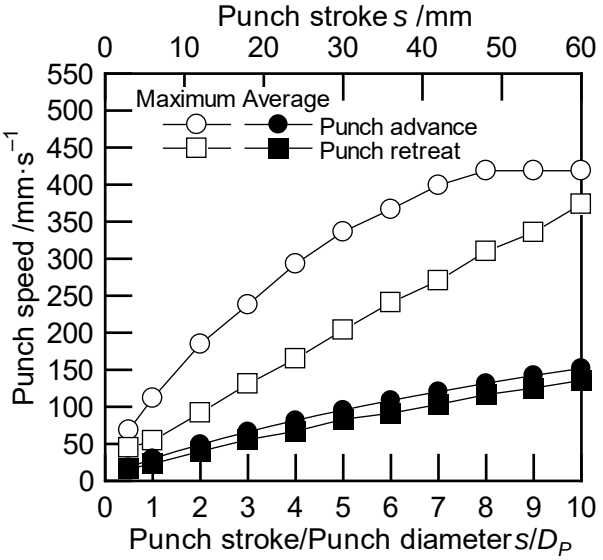


Fig. 4 Maximum and average punch speeds–stroke diagram for the advance and retreat ram motions on a servo press (Komatsu Industrial Corp., H1F45).

### 2.3. Amount of lubricant sucked into the cavity by the retreat of the punch

The amount of lubricant sucked into the cavity was estimated from the weight changes in the specimen including the lubricant before and after the retreat of the punch on the assumption that the sucked lubricant adhered to the surface of the hole. Figure 5 shows the measured volume ($V_{Lub}$) and the nominal thickness ($h_{Lub}$) of the lubricant sucked through the internal channel into the cavity. The nominal thickness of sucked lubricant was estimated by dividing the sucked volume by the surface area of the cavity, as given in the following equation:

$$h_{Lub} = (V_{Lub}/(\pi(D_P/2)^2+\pi D_P s_r)) \quad (1)$$

The volume of sucked lubricant increases with increases in the retreat stroke. The nominal thickness of the sucked lubricant was estimated to be greater than 50 μm when the retreat stroke of the punch ($s_r/D_P$) is longer than 0.5. The maximum thickness of lubricant trapped between the punch and the specimen during forming ($h_{Trap}$) was calculated to be approximately 2.8 μm with the following equation (Oyane and Osakada, 1969),

$$h_{Trap} = \sqrt[3]{3\eta u (D_P / 2)^2 / P} \tag{2}$$

where $\eta$ is the viscosity of the lubricant (= 27.1 mPa·s at 40 ºC), $u$ is the forming speed (= 50 mm/s), and $P$ is the forming pressure (= 1.7 GPa, see Fig. 12). By comparing the nominal thickness ($h_{Lub}$) and the maximum trapped thickness ($h_{Trap}$), it can be seen that sufficient lubricant to reduce the friction is sucked through the internal channel into the forming zone for retreat actions of $s_r/D_P \geq 0.5$. Thus, the retreat stroke was fixed at $s_r/D_P = 1.0$ in this study.

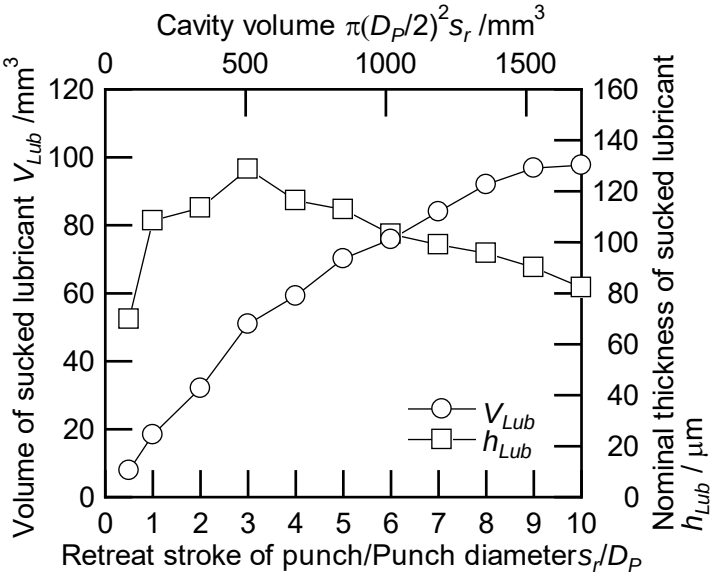


Fig. 5 Relationship between the retreat stroke of the punch and the volume of lubricant sucked into the cavity.

**3. Finite element analysis conditions**

To analyze the experimental results for the accuracy of the shape of the formed hole, a finite element simulation was carried out. A rigid-plastic finite element method for plastic deformation (Osakada et al., 1982; Osakada and Mori, 1985) and a heat conduction finite element method for temperature changes were employed to calculate the stress, strain states, and temperature distribution of the specimen at each calculation step of the backward

extrusion. In the method, the material was assumed to obey the yield criterion on the basis of the plasticity theory for a slightly compressive material, and the stress components were calculated directly from the strain rate components. The constitutive relation used in this study was multilinear isotropic hardening, as determined from the flow stress curves shown in Fig. 6. The flow stress–equivalent strain relations at every 0.05 of equivalent strain were used as input data for the finite element analysis. The temperature dependences of the flow stress curves were obtained by linear interpolation. The average flow stress for the AA6061-T6 aluminium alloy was obtained at various temperatures from the load-stroke data in the upsettability test (Osakada et al., 1981). The average flow stress and average equivalent strain were calculated by a finite element simulation from the measured load and reduction in height in the experiment.

A two-dimensional axisymmetric analysis was conducted as shown in Fig. 7. The dimensions, geometries, and initial temperatures of each specimen and the tools used in the simulation were identical to the experimental values. The initial element shape was rectangle in 667 μm x 667 μm. The elements were automatically remeshed as rectangle or triangle element with appropriate sizes. The heat transfer coefficients for the specimen-tool contact interfaces and the free surfaces were determined with heating and cooling tests to be 5000 $W \cdot m^{-2} \cdot K^{-1}$ and 20 $W \cdot m^{-2} \cdot K^{-1}$, respectively. Although the friction condition is affected by the sucked amount of the lubricant during the retreat motion of the punch, the influences of friction on the forming load and deformation of the specimen under these extrusion conditions were found to be small, as shown in section 4.3. The frictional condition of the specimen-tool interface was assumed to be specified by the coefficient of shear friction $m$ = 0.20, irrespective of the punch motion.

In this study, the accuracy of the shape of the formed hole was not directly analysed in the finite element simulation because elastic-plastic finite element analysis is necessary to

calculate the shape of the formed hole with high accuracy in a finite element simulation. Various material properties of the specimen and dies such as the stress-strain relation and the thermal conductivity were required as input data for the elastic-plastic finite element simulation. Furthermore, the temperature dependences of these properties were required to be considered. For these reasons, the changes in the temperature distributions of the aluminium specimens during forming were the focus of the simulations because the changes strongly affect shape accuracy of the forged specimen (Ishikawa et al., 2000; Ishiguro et al., 2010).

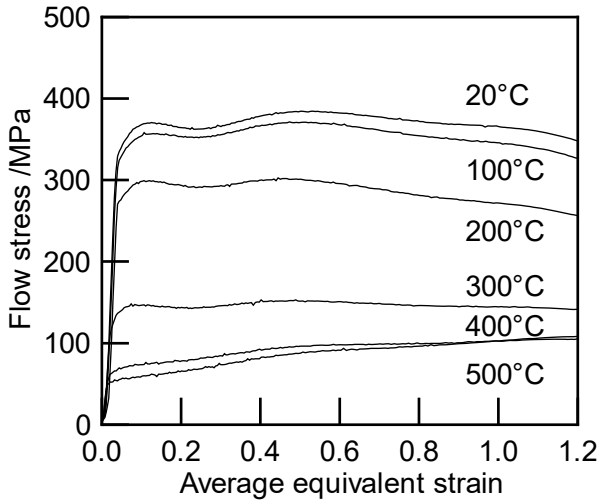


Fig. 6 Flow stress curves of the AA6061-T6 aluminium alloy measured by upsettability test.

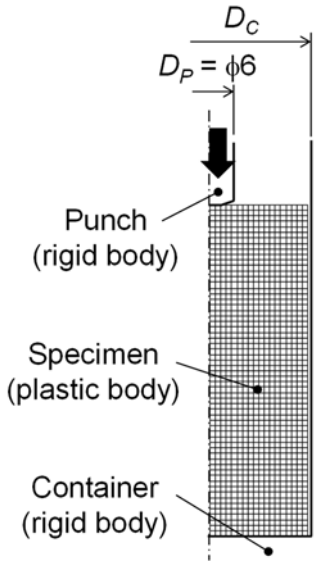


Fig. 7 Two-dimensional axisymmetric analysis model of hole forming for finite element analysis.

## 4. Experimental results

### 4.1. Boss at the bottom of the formed hole

A boss is formed at the centre of the bottom of the formed hole by the internal channel of the punch. The relationship between the formed boss height and the punch motion is plotted in Fig. 8. Irrespective of the punch motion, the boss height increases with increasing in the total punch stroke. If a valve for preventing backward material flow is placed at the end of the internal channel, the boss height may be reduced.

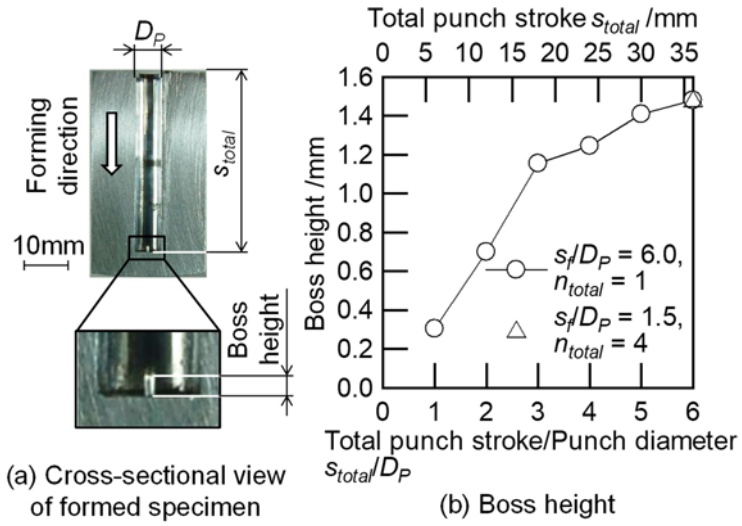


Fig. 8 Height of the boss at the bottom of the hole in the aluminium specimen (extrusion ratio $R$ = 1.07).

### 4.2. Punch motion for the prevention of galling

Figure 9 shows the surface profiles of the sidewall part of the formed hole measured by a 3D laser scanning microscope. Galling is observed in the conventional forming method ($s_f/D_P$ = 6.0, $n_{total}$ = 1), while smooth surface without galling is obtained in the proposed forming method ($s_f/D_P$ = 1.5, $n_{total}$ = 4). Figure 10 shows the roughness of the surface of the formed hole. The surface roughness was measured in circumferential direction of the formed hole by a stylus type surface roughness tester. The galling of the hole surface is caused by the sliding of the punch during the advance and/or retreat of the punch. The occurrence of the galling was assumed in this study as roughness larger than $Ra$ = 0.4 μm from the surface roughness and visual inspection of the formed hole.

The relationship between the forming stroke of the punch in each forming step and the occurrence of galling is summarized in Fig. 11. When the extrusion ratio increases, the critical forming stroke for the prevention of galling becomes shorter because severe sliding occurs between the punch sidewall and the specimen at high extrusion ratios. These results confirm that the proposed forming method with appropriate pulse ram motions effectively

prevents specimen from galling. Furthermore, a deeper hole with a smooth surface (no galling) can be ideally formed by using pulse ram motions if the appropriate punch motions are repeated. The maximum depth of the hole (forming limit) was estimated to be approximately 20 of the aspect ratio (hole depth/diameter) in the proposed pulse forming of an AA6061 aluminium specimen when the buckling and strength of the punch were taken into account (Matsumoto et al., 2011). However, the forming of a deeper hole was difficult to carry out in this study due to the specifications of the press.

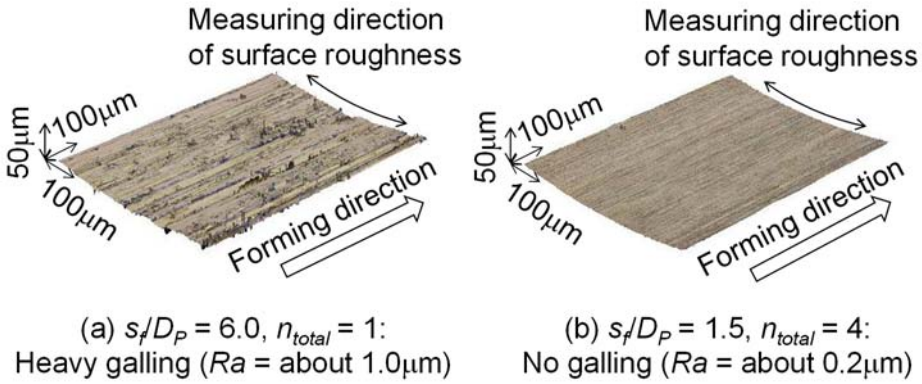


(a) $s_f/D_P$ = 6.0, $n_{total}$ = 1:
Heavy galling (*Ra* = about 1.0μm)

(b) $s_f/D_P$ = 1.5, $n_{total}$ = 4:
No galling (*Ra* = about 0.2μm)

Fig. 9 Surface profiles of the side wall of the formed hole measured by 3D laser scanning microscope.

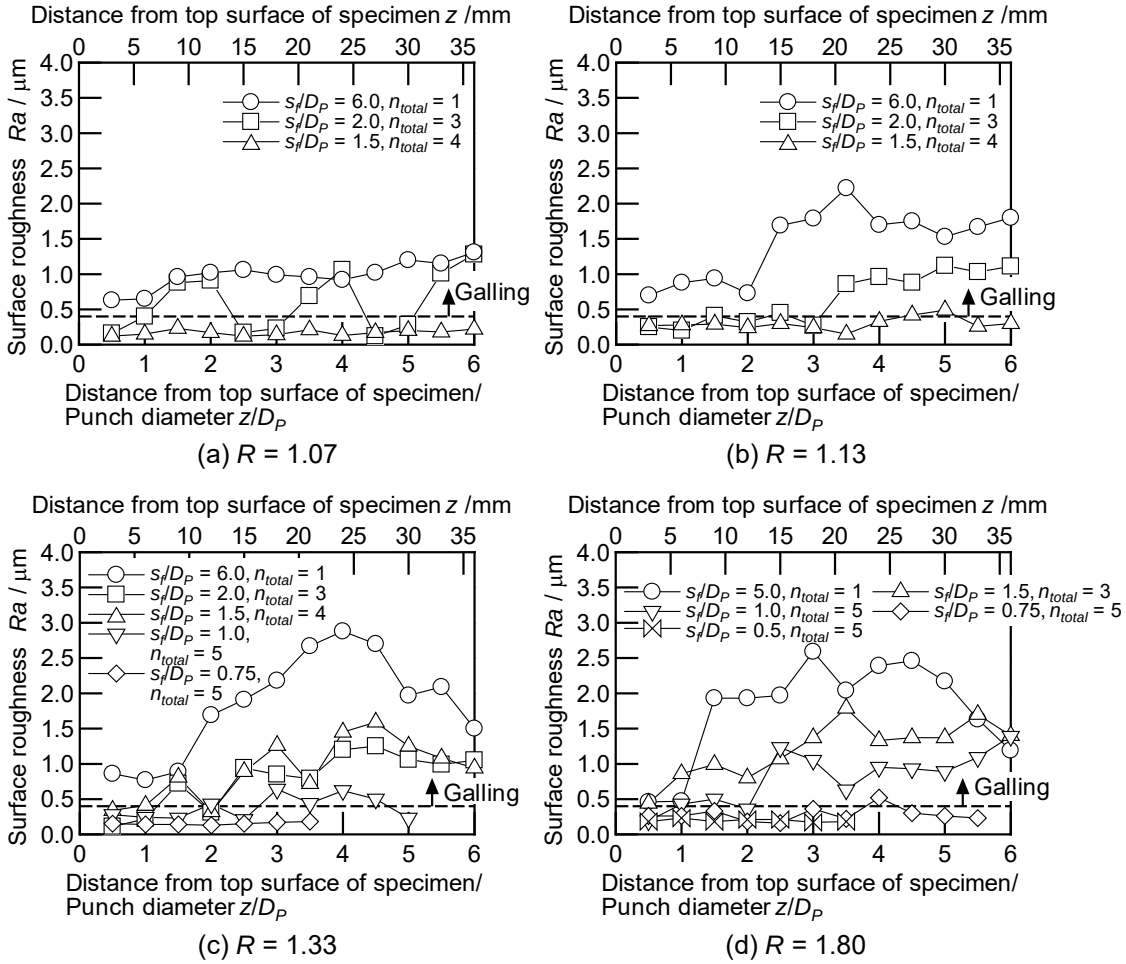


Fig. 10 Influence of punch motion on the surface roughness of the formed hole ($s_r/D_P$ = 1.0).

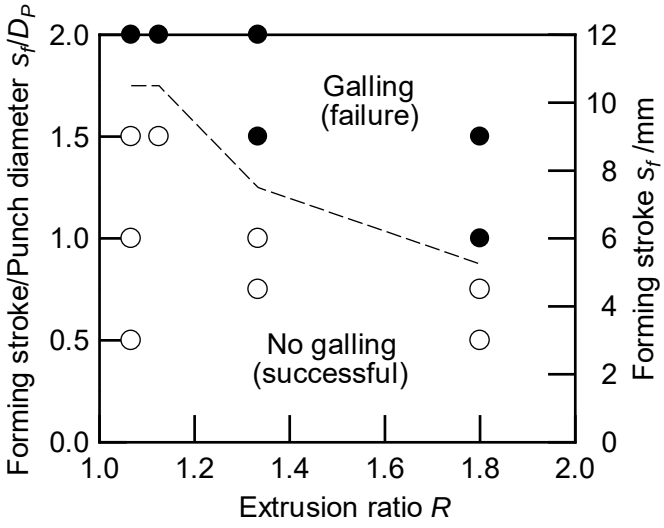


Fig. 11 Relationship between the forming stroke of the punch in each forming step and the occurrence of galling ($s_r/D_P$ = 1.0).

### 4.3. Forming load

Figure 12 shows the forming pressure–stroke diagram for the forming of an AA6061 aluminium specimen with pulse ram motion. The nominal forming pressure ($P$) was calculated that the forming load was divided by the cross-sectional area of the punch ($\pi(D_P/2)^2$). Although sufficient lubricant was periodically supplied into the formed hole cavity before every forming step, the forming load is not sensitive to the lubricating condition. However, since severe plastic deformation results at high extrusion ratios, the specimen temperature increases due to heat generation. Thus the forming pressure decreases with increases in the extrusion ratio.

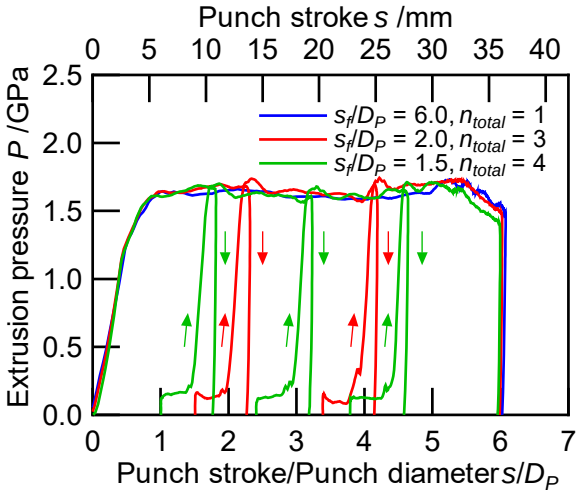


(a) $R$ = 1.07

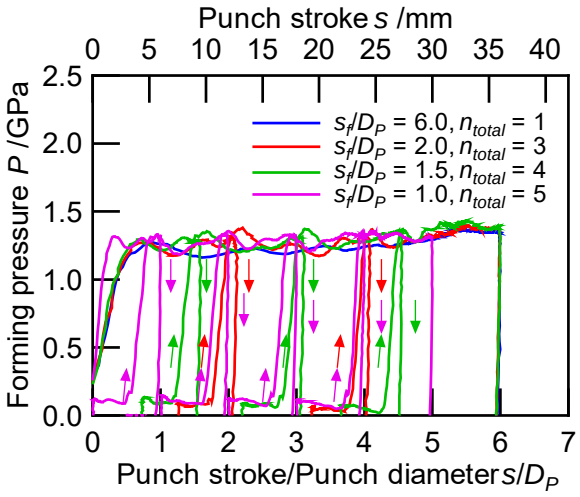


(b) $R$ = 1.33

Fig. 12 Forming pressure–stroke diagram for the forming of an AA6061 aluminium specimen with pulse ram motion ($s_r/D_P$ = 1.0).

### 4.4. Accuracy of the shape of the formed hole

To examine the accuracy of the shape of the formed hole, the diameter and the centre position of the formed hole were measured for every $s$ = 3 mm ($s/D_P$ = 0.5) in the depth direction of the hole by a measuring microscope. The accuracy of the microscope was 1 μm. Figure 13 shows the diameter distributions of the formed holes for the proposed and conventional forming methods with $s_{total}/D_P$ = 6.0, $R$ = 1.07. The variation in the hole

diameter obtained with the conventional forming method ($s_f/D_P$ = 6.0, $n_{total}$ = 1) is larger than that obtained with the proposed forming method ($s_f/D_P$ = 1.5, $n_{total}$ = 4); note especially that the differences between the hole and punch diameters are large at the bottom and top positions for the conventional forming method. Although the causes are difficult to specify, this may be caused from the difference of the contacting speed of the punch to the specimen between the conventional and proposed forming methods. Because the servo press is driven through a mechanical link, the ram speed decreases toward the end position of the 1st forming step in the proposed method. Due to this, the contacting speed of the punch to the top surface of the specimen in the conventional method is faster than that in the proposed method. In this study, the contacting speeds of the conventional ($s_f/D_P$ = 6.0, $n_{total}$ = 1) and proposed ($s_f/D_P$ = 1.5, $n_{total}$ = 4) methods are about 220 mm/s and 100 mm/s, respectively. Furthermore, there is tolerance of diameter of the specimen and container. The high contacting speed of the punch to the specimen causes unstable deformation at the early stage of the forming. Thus the shape accuracy of the formed hole in the conventional method may be inferior to that in the proposed method. The standard deviations ($\sigma_d$) of the diameter distributions for forming with the two methods for $s_{total}/D_P$ = 6.0 are shown in Fig. 14. $\sigma_d$ was calculated with the following equation,

$$\sigma_d = \sqrt{\frac{1}{n}\sum_{i=1}^{n}\left(d_i - d_{avg}\right)^2} \tag{3}$$

where $d_i$ is the diameter of the formed hole at position $i$ and $d_{avg}$ is the average diameter of the formed hole. Irrespective of the extrusion ratio, the standard deviation obtained with the proposed forming method ($s_f/D_P$ = 1.5, $n_{total}$ = 4) is smaller than that obtained with the conventional forming method ($s_f/D_P$ = 6.0, $n_{total}$ = 1).

Figure 15 shows the centre position distributions for the formed holes of the two methods with $s_{total}/D_P$ = 6.0, $R$ = 1.07. There is no large difference between the distributions

obtained with the proposed and conventional forming methods. The standard deviations ($\sigma_a$) of the centre position distributions in forming with the two methods for $s_{total}/D_P$ = 6.0 are shown in Fig. 16. The standard deviation obtained with the proposed forming method is slightly smaller than that obtained with the conventional forming method. These results show that a hole with high shape accuracy was obtained with the proposed forming method.

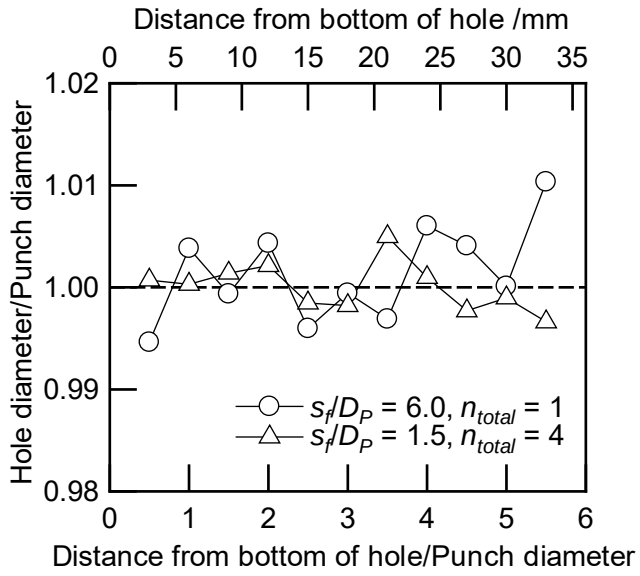


Fig. 13 Distributions of the diameters of the formed holes ($s_{total}/D_P$ = 6.0, $R$ = 1.07).

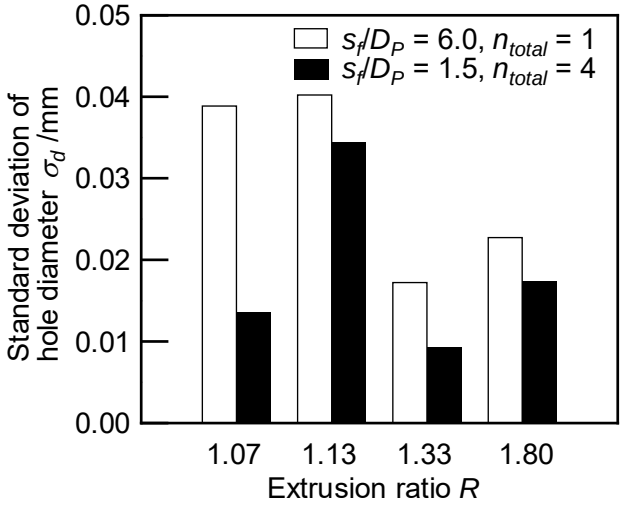


Fig. 14 Standard deviations of the diameters of the formed holes ($s_{total}/D_P$ = 6.0).

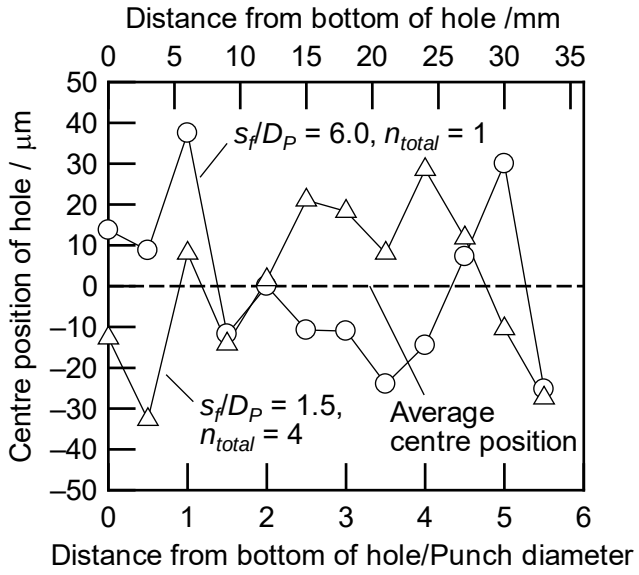


Fig. 15 Distributions of the centre positions of the formed holes ($s_{total}/D_P$ = 6.0).

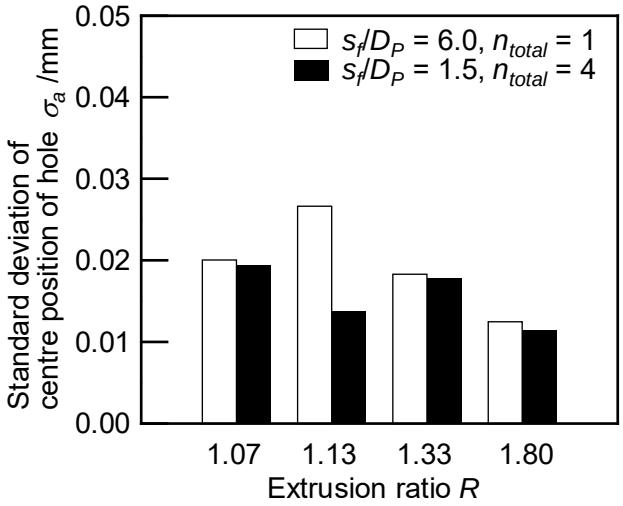


Fig. 16 Standard deviations of the centre positions of the formed holes ($s_{total}/D_P$ = 6.0).

## 5. Discussion on the accuracy of the shape of the formed hole

Shape accuracy of the formed specimen is complexly determined by many forming parameters. Since the parameters that are crucial to the shape accuracy of the proposed forming method are considered to be lubrication and the temperature changes in the specimen during forming, the shape accuracy of the formed hole is individually discussed from viewpoints of the lubrication and temperature change.

Since the lubrication state is maintained at a stable level until when the forming of a deep hole is finished in the proposed forming method with the appropriate punch motions, seizure at the punch surface and galling at the hole surface can be prevented. Seizure and galling are naturally expected to degrade the accuracy of the shape of the formed hole.

The calculated temperature distributions of the aluminium specimen during hole forming are shown in Fig. 17. The temperature around the punch corner is raised due to heat generation by plastic deformation. The temperature distribution is strongly affected by the punch motion. Figure 18 shows the changes in the maximum, average, and minimum calculated temperatures of the aluminium specimen during hole forming. The average and minimum temperatures of the specimen are hardly affected by the punch motion, whereas the maximum temperature of the specimen is strongly affected by the punch motion. The maximum temperature during the pulse punch motions is lower than that arising during the conventional forming method ($s_f/D_P$ = 6.0, $n_{total}$ = 1). In the pulse punch motions, backward extrusion is carried out with interruptions because the punch is pushed into the specimen in a manner that combines pulsed and stepwise modes. Due to these interruptions, the maximum temperature drops periodically during the punch retreat at every forming step, and thus increases in the specimen temperature are prevented. The maximum temperature is found near the bottom of the hole, although the volume with this maximum temperature accounts for less than 10% of the whole volume of the specimen. No large change in the average temperature of the specimen is seen by the punch motions, as shown in Fig. 18. As a result, no large difference of the forming load during punch advance is also seen by the punch motions, as shown in Fig. 12.

The standard deviations ($\sigma_T$) of the temperature distributions in forming for $s_{total}/D_P$ = 6.0 are shown in Fig. 19. $\sigma_T$ was calculated with the following equations,

$$\sigma_T = \sqrt{\frac{1}{n}\sum_{i=1}^{n}\left(T_i - T_{avg}\right)^2} \tag{4}$$

$$T_{avg} = \sum_{i=1}^{n} T_i V_i \Big/ \sum_{i=1}^{n} V_i \tag{5}$$

where $T_i$ is the temperature of the specimen at element $i$, $T_{avg}$ is the average temperature of the specimen, and $V_i$ is the volume of the specimen at element $i$. The standard deviation in the pulse punch motion is less than that of the conventional forming method ($s_f/D_P$ = 6.0, $n_{total}$ = 1). The formed product with low heterogeneous temperature distribution is found to be obtained in the proposed forming method.

In general, thermal deformation due to air cooling occurs heterogeneously after forming in the formed specimen with heterogeneous temperature distribution. In addition, when the specimen temperature is partially raised by heat generation during forming, plastic deformation tends to localize in the higher temperature regions of the specimen because flow stress is reduced at higher temperatures. For these reasons, we conclude that the proposed forming method provides a formed product with high shape accuracy.

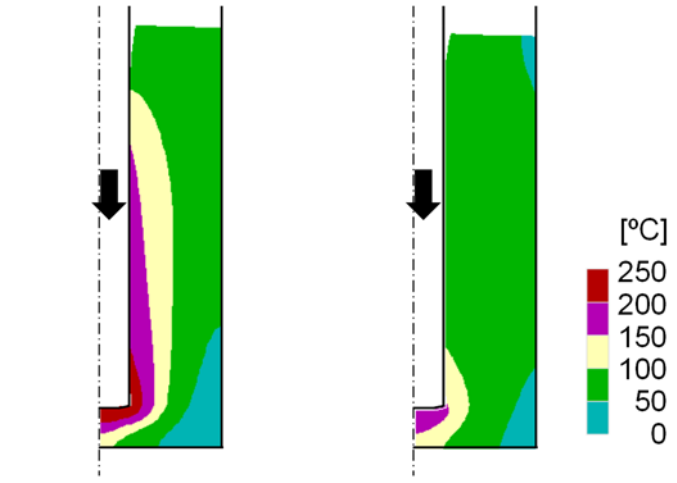


Fig. 17 Temperature distributions of the aluminium specimen during hole forming ($R$ = 1.07) (finite element simulation).

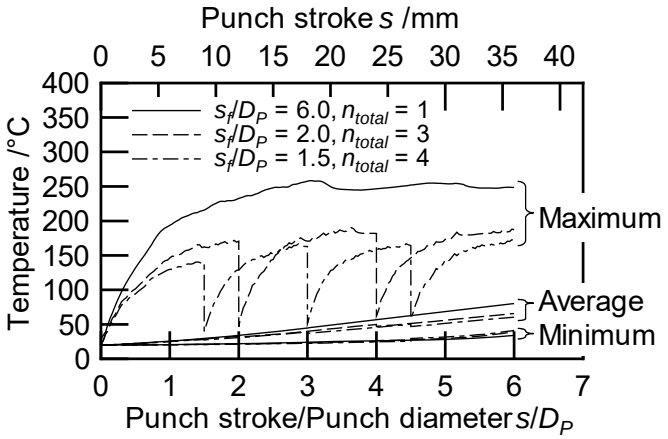


(a) $R$ = 1.07

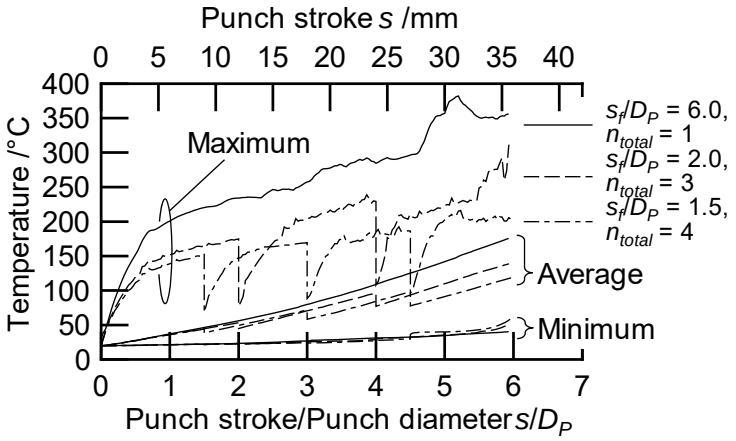


(b) $R$ = 1.33

Fig. 18 Changes in the maximum, average, and minimum temperatures of the aluminium specimen during hole forming (finite element simulation).

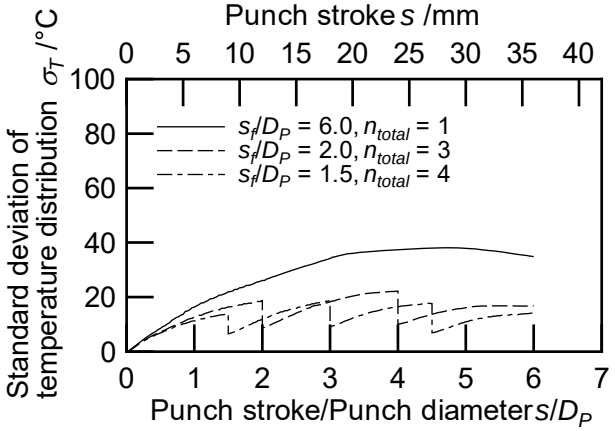


(a) $R$ = 1.07

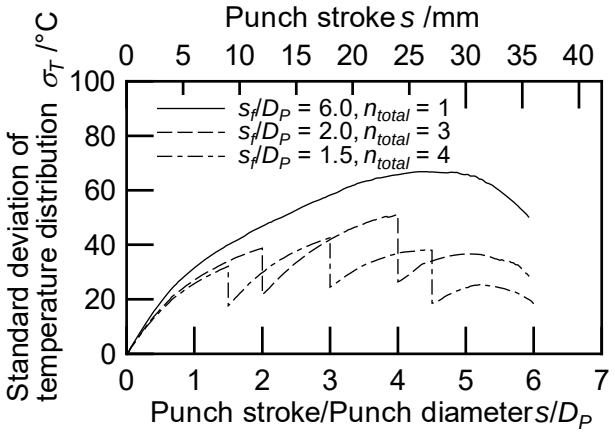


(b) $R$ = 1.33

Fig. 19 Changes in the standard deviations of the temperature distributions of the aluminium specimens during hole forming (finite element simulation).

## 6. Conclusions

The appropriate punch motions for prevention of galling of the formed hole for extrusion ratios in the range 1.07–1.80 were investigated with the proposed forming method using a servo press. The accuracy of the shape of the formed hole with the proposed forming method was examined and discussed in terms of lubrication and temperature changes through the experimental finite element simulation results. The following conclusions were obtained.

1) Sufficient liquid lubricant to prevent the galling of the aluminium specimens is

periodically supplied to the deforming zone through the internal channel by retreat strokes of the punch longer than 3 mm for a punch diameter of 6 mm.

2) When the retreat stroke is fixed as 6 mm for a punch diameter of 6 mm, the forming strokes that prevent galling of the aluminium specimens at each forming step are those shorter than 9 mm (extrusion ratio: 1.07), 9 mm (1.13), 6 mm (1.33), and 4.5 mm (1.80).
3) The proposed forming method can control the temperature changes in specimens during forming as well as maintain good lubrication between the punch and the specimen. As a result, the proposed forming method provides a formed product with high shape accuracy because the formed product with low heterogeneous temperature distribution is obtained.

**Acknowledgements**

The authors would like to thank Dr. K. Osakada, Emeritus professor of Osaka University for his valuable advice. The authors also would like to thank DIJET Industrial Co., Ltd. and Nichidai Corporation for providing the cemented carbide punch and tool steel dies used in this study. This study was financially supported in part by the Japan Ministry of Education, Culture, Sports, Science and Technology with a Grant-in-Aid for Young Scientists (B) and by the Light Metal Educational Foundation, Inc.

**References**

- Ernst, M., 2011, Servo forming is more than a trend. Steel Research International. 82 Special Edition: 10th International Conference on Technology of Plasticity, ICTP2011, 49-55.
- Groche, P., Scheitza, M., Kraft, M., Schmitt, S., 2010, Increased total flexibility by 3D servo presses. CIRP Annals - Manufacturing Technology. 59(1), 267-270.
- Ishiguro, T., Yoshimura, M., Yoshida, Y., Yukawa, N., Ishikawa, T., 2010, Influence of

slide motion on dimensional accuracy in cold backward extrusion by using servo press. Steel Research International. 81(9) Special Edition, 410-413.

- Ishikawa, T., Yukawa, N., Yoshida, Y., Kim, H., Tozawa, Y., 2000, Prediction of dimensional difference of product from tool in cold backward extrusion. CIRP Annals - Manufacturing Technology. 49(1), 169-172.
- Maeno, T., Osakada, K., Mori, K., 2011, Reduction of friction in compression of plates by load pulsation. International Journal of Machine Tools and Manufacture. 51(7-8), 612-617.
- Matsumoto, R., Sawa, S., Utsunomiya, H., Osakada, K., 2011, Prevention of galling in forming of deep hole with retreat and advance pulse ram motion on servo press. CIRP Annals - Manufacturing Technology. 60(1), 315-318.
- Osakada, K., Kawasaki, T., Mori, K., 1981, A method of determining flow stress under forming conditions. CIRP Annals - Manufacturing Technology. 30(1), 135-138.
- Osakada, K., Mori, K., 1985, The use of micro- and supercomputers for simulation of metal forming process. CIRP Annals - Manufacturing Technology. 34(1), 241-244.
- Osakada, K., Mori, K., Altan, T., Groche, P., 2011, Mechanical servo press technology for metal forming. CIRP Annals – Manufacturing Technology. 60(2), 651-672.
- Osakada, K., Nakano, J., Mori, K., 1982, Finite element method for rigid-plastic analysis of metal forming – formulation for finite deformation. International Journal of Mechanical Sciences. 24(8), 459-468.
- Oyane, M., Osakada, K., 1969, The mechanism of lubricant trapping under dynamic compression. Bulletin of JSME. 12(49), 149-155.
- Wang, X.Y., Yukawa, N., Yoshida, Y., Suke, T., Ishikawa, T., 2009, Research on some basic deformations in free forging with robot and servo-press. Journal of Materials Processing Technology. 209(6), 3030-3038.

- Weinert, K., Inasaki, I., Sutherland, J.W., Wakabayashi, T., 2004, Dry machining and minimum quantity lubrication. CIRP Annals – Manufacturing Technology. 53(2), 511-537.